Protoplanetary Disks and embedded Planets

Wilhelm Kley

Institut für Astronomie & Astrophysik
Abtlg. Computational Physics
Auf der Morgenstelle 10, 72076 Tübingen
wilhelm.kley@uni-tuebingen.de

Abstract

After its formation a planetary embryo of a few earth masses is still surrounded by the protoplanetary disk material. Gravitational interaction of this embedded protoplanet with the disk material leads to a change of its orbital elements, most notably its semi-major axis (the change of which is referred to as migration) and eccentricity. In this contribution we describe the main aspects of these processes.

Depending on the mass of the planet and on the properties of the disk it is possible to classify into different types of migration. In the first case, for low planetary masses in laminar disks, the interaction is linear and can be treated by semi-analytical methods. This leads to a simple estimate for the migration rate, so called Type I migration, studied long before the discovery of the first extra-solar planet. In the second case, for large planetary masses, the interaction is non-linear, the planet wake becomes a shock in the vicinity of the planet location and opens an annular gap at the planet orbit. In this regime numerical methods are used to analyse the torques acting on the planet, yielding the so called Type II migration. In this review the setup of such models and the main results of these multi-dimensional numerical hydrodynamic simulations are described and presented.

One major observational evidence for the migration scenario are resonant systems. The resonances have been most likely established by converging differential migration of the planets leading to capture into the resonances. A problem with this scenario is that continued migration of the system while it is trapped in the resonances leads to orbital eccentricities that rapidly exceed the observational upper limits for system such as GJ 876. Detailed numerical simulations are described to explain this discrepancy.

1 Introduction

The formation of planets is intimately connected with the occurrence of disks around young stars. Similar to the scenario outlined already by Kant and Laplace, we know

Reviews in Modern Astronomy 19. Edited by S. Röser

ISBN: 3-527-40662-X

today that planets form from material orbiting a central proto-star in a flattened disk-shaped configuration. These disks, called either circumstellar, protostellar, or protoplanetary disk depending on the point of view, consist of the gas and dust left behind during the star formation process due to angular momentum conservation. Within the disk, gas and dust accumulate to eventually become a planet. There is strong evidence that our own Solar System was born from such a disk - the protosolar nebula - 4.6 billion years ago.

Directly after the discovery of the very first extrasolar planets around main sequence stars it has become obvious that the new planetary systems differ substantially from our own Solar System. Amongst other properties one distinguishing feature is the close proximity of several planets to their host stars (hot Jupiters). As it is difficult to imagine scenarios to form planets so close the their parent star it is generally assumed that massive, Jupiter like planets form further away, and then migrate inwards towards the star due to disk-planet tidal interactions. Hence, the mere existence of hot Jupiters can be taken as clear evidence of the occurrence of migration. Interestingly, theoretically the possibility of migrating planets has long been predicted already in the early eighties of the last century.

Another observational indication that some migration of planets must have occurred is the existence of planets in mean motion resonances. Due to converging differential migration of two planets both embedded in a protoplanetary disk they can be captured in a low order mean motion resonance. The most prominent example is the system GJ 876 where the planets have orbital periods of roughly 30 and 60 days.

Here, in this review we focus on the theoretical aspects of disk-planet interaction which leads to a change in the orbital elements of the planet most notably its semi-major axis. We treat systems with a single planet and do also consider planetary systems containing multiple resonant planets.

2 Protoplanetary Disks

Observational evidence of the existence of protoplanetary disk has become conclusive in recent years. Detailed multi-dimensional radiative models of disks allow to extract information on structure, and evolution of such disks. We summarize very briefly some important results on the observational as well the theoretical aspects of such disks.

2.1 Observational evidence

Indirect observational evidence for the presence of non-spherical structures around young solar-type stars came first from sub-millimeter and infrared observations (Strom et al. 1989), asymmetric scattering of visual and near-infrared light (Zinnecker et al. 1999), line profiles (Edwards et al. 1987), and the detection of stellar jets. Typically a far-IR and submm excess in the SED is attributed to the presence of circumstellar material. Most surveys imply that more than half of the youngest low-mass pre-main sequence stars (1–3 Myrs) are associated with disks. As most stars

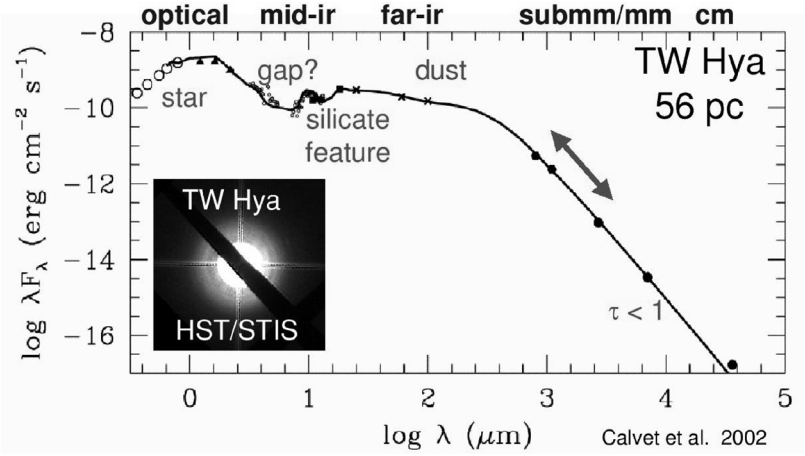

Figure 1: Spectral energy distribution for TW Hya from the optical to cm wavelength. The origin of the different contributions to the spectrum are indicated. The extended emission at longer wavelength is indicative for a circumstellar dust-disk, and the indentation in the mid-IR range for a hole in the center of the disk (after Calvet et al. (2002)).

are born in associations, circumstellar disks rarely evolve in isolation and gravitational interactions can influence the disk structure, its evolution and life-time. This will influence the likelihood for the formation of planetary systems. Another limiting factor is photo-evaporation of disks due to irradiation of nearby massive stars.

With the progress in imaging sensitivity provided by the HST in space and adaptive optics at large telescopes and millimeter interferometry from the ground, direct images of disks could be obtained (McCaughrean et al. 2000; Wilner & Lay 2000), and Keplerian rotation curves be measured.

Planet formation takes time (Lissauer 1993), and as such requires a nursing environment available for a sufficiently long time, i.e. long-lived circumstellar disks. From infrared observations of the dust grain emission the lifetime of protoplanetary disks has been estimated to be $\lesssim$10 million years (Briceño et al. 2001). However, the problem of using the dust as a probe of the gas mass in disks (and hence their ages) lies in the uncertain knowledge of the dust grain growth and its timescales. A decrease in disk luminosity can also be attributed to the fact that dust grains grow to planetesimals and larger bodies. There are at least a number of indications that some of the gas stays as long as a few 10 Myr in circumstellar disks.

2.2 Theoretical models

Protostellar disks are typically considered to be accretion disks. Simple disk models parameterize the radial distribution by power laws eg. for density and temperature, and calculate theoretical SEDs by adding up black-body contributions from all annuli. Early models of protoplanetary disks have assumed thin disks, in which the energy is generated solely by internal viscous heating (Lin & Papaloizou 1980;

Bell & Lin 1994). Then it has been recognized that temperature distributions could been fitted better by assuming passive accretion disks in which a substantial fraction of the emitted energy comes from the heating by irradiation from the central star. Purely passive models for Herbig Ae/Be stars have been calculated by Hartmann et al. (1993), and in two-dimensions by Chiang & Goldreich (1997).

Two-layer models are frequently used to construct accretion disks consisting of a central part near the equatorial plane which is viscously heated and a surface layer which intercepts the radiation received by the central protostar (D'Alessio et al. 1998, 1999). More recently these models have been extended to include effects of a hot irradiated inner rim of the accretion disk (Dullemond et al. 2001). An analysis of existing two-dimensional disk models with respect to their applicability to fitting observed SEDs has been performed by Dullemond & Natta (2003). Using these disk models having several different components it has been possible to obtain much better fits to the observed spectra.

From HST observations of protostellar disks in Orion at different wavelengths a continuous wavelength-size relationship has been inferred, indicating thinner disks at longer wavelengths. This has been interpreted as evidence for grain growth in such disks (Shuping et al. 2003). Indication of grain growth has also been seen in the circumstellar disk of the butterfly star in Orion (Wolf et al. 2003). Evidence for the formation of silicates which play an important role during planet formation, has been obtained in several cases. Silicate features are present for example in observed SEDs (refer to Fig. 1) or can be directly seen in higher resolution spectra obtained for example with the ISO satellite (Malfait et al. 1998).

3 Disk-Planet Interaction

Having mentioned some observational indications that formation and growth of planetary precursor material is in fact possible in protoplanetary disks we jump now directly to the end-phase of planet formation and study the physics of disk-planet interactions. For that purpose we assume that the protoplanet has formed already but is still embedded in its gaseous environment. A detailed review on this topic has recently been given by Masset & Kley (2005) and we concentrate here only on the major results.

3.1 Linear Analysis: Type I migration

The problem of determining the impact of tidal effects on the evolution of the planet orbit amounts to an evaluation of tidal torques. For smaller mass planets the ambient disk structure will be perturbed only weakly and a linear analysis where the planet is considered as a perturbation to the basic (axisymmetric) disk structure is sufficient. The dependence on the azimuthal angle φ of the gravitational potential ψ of the planet is decomposed into a Fourier series

$$\psi(r,\varphi,t) = \sum_{m=0}^{\infty} \psi_m(r)\cos\{m[\varphi-\varphi_p(t)]\}, \qquad (1)$$

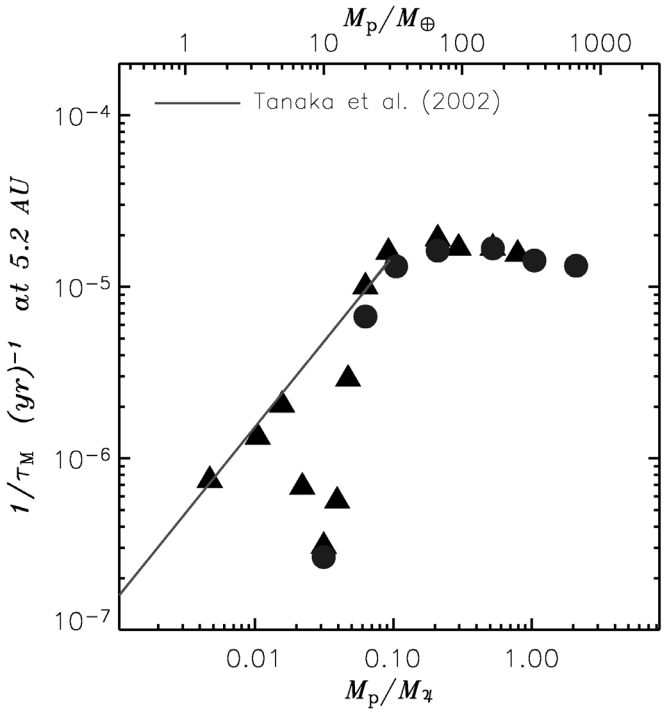

Figure 2: The inverse migration rate for different planet masses for 3D fully non-linear nested grid simulations. The symbols denote different approximations (smoothening) for the potential of the planet. The solid line refers to linear results for Type I migration by Tanaka et al. (2002), see Eq. (2). Figure adapted from D'Angelo et al. (2003).

where $\varphi_p = \Omega_p t$ is the azimuth angle of the planet. The total torque acting on the disk is given by $\Gamma = \int_{Disk} \Sigma \vec{r} \times \nabla \psi d^2 r$ where Σ is the surface density of the disk.

An m-folded external forcing potential $\psi_m(r, \varphi)$ which rotates with a pattern frequency Ω_p in a disk with angular velocity profile $\Omega(r)$ triggers a response wherever the potential frequency as seen in the matter frame $\omega = m(\Omega - \Omega_p)$ matches either 0 or $\pm\kappa$ (κ being the epicyclic frequency), i.e. when it is in phase with a natural oscillation frequency of the material in the disk. The first case corresponds to a co-rotation resonance (since it implies $\Omega = \Omega_p$, hence fluid elements corotate with the forcing potential) while the second case corresponds to a Lindblad resonance (outer Lindblad resonance for $\omega = \kappa$ and inner Lindblad resonance for $\omega = -\kappa$), where the potential forcing is in phase with the epicyclic motion of the disk particle. The derivation of these resonant torques in the context of satellite(planet)-disk interaction can be found in Goldreich & Tremaine (1979); Papaloizou & Lin (1984) or Meyer-Vernet & Sicardy (1987). In a Keplerian disk, the torque exerted on the disk by the external planetary potential is positive at an outer Lindblad resonance, and negative at an inner Lindblad resonance, i.e. the planet repels the disk. The planet in turn feels a negative torque from the outer resonances and a positive torque from the

inner ones. Summation over all components m of the potential leads to a *negative total Lindblad torque* implying that the planet *migrates inward* (Ward 1986, 1997).

The magnitude of the corotation torques amount typically to only a few percent of the Lindblad torques (Ward 1997; Tanaka et al. 2002). There is a number of estimates of this *linear regime* of migration, called *Type I migration*, in the literature (see Ward (1997) and refs. therein). The most recent linear calculations by Tanaka et al. (2002) take into account 3D effects, and are based upon the value of the total tidal torque, including the corotation torque, and is given by

$$\tau \equiv a/\dot{a} = (2.7 + 1.1\alpha)^{-1} q^{-1} \frac{M_*}{\Sigma a^2} h^2 \Omega_p^{-1}, \tag{2}$$

for a surface density profile $\Sigma \propto r^{-\alpha}$. For an Earth-mass planet around a solar mass star at $r = 1$ AU, in a disk with $\Sigma = 1700$ g cm^{-2} and $h = 0.05$, this translates into $\tau = 1.6 \cdot 10^5$ years.

This analytical estimate has been verified by means of 3D numerical simulations (Bate et al. 2003; D'Angelo et al. 2003). Both find an excellent agreement in the limit of low-mass, thus they essentially validate the linear analytical estimate. However, while Bate et al. (2003) find agreement with the linear results for all planet masses, D'Angelo et al. (2003) results give very long migration rates for intermediate masses, i.e. for Neptune-sized objects (see Fig. 2). Additional 2d and 3D high resolution numerical simulations by Masset et al. (2006) show that this *migration excess* from the linear results is a robust phenomenon whose strength varies *i)* with departure from the $\Sigma \propto r^{-3/2}$ relation, *ii)* with the value of the viscosity, and *iii)* with the disk thickness. The transition from linear to the excess regime is caused apparently by the onset of non-linear effects.

The type I migration time scale is very short, much shorter than the build up time of the $M_p \sim 5 - 15\ M_\oplus$ solid core of a giant planet. Hence, type I migration constitutes a bottleneck for the accretion scenario for these massive cores. To date this remains an unsolved problem (see the discussion in the recent work by Alibert et al. (2004); Papaloizou & Nelson (2005)). However, the aforementioned *excess* and effects due to fully turbulent magnetic disks (Nelson & Papaloizou 2003, 2004), called *stochastic* migration may assist in resolving this timescale problem.

3.2 Numerical Simulations: Type II migration

When the planet grows in mass the disk response cannot be treated any longer as a linear perturbation. The perturbation becomes non-linear and the planetary wake turns into a shock in its vicinity. Dissipation by these shocks as well as the action of viscosity leads to the deposition of angular momentum, which pushes material away from the planet and a gap opens. The equilibrium width of the gap is determined by the balance of gap-closing viscous and pressure forces and gap-opening gravitational torques.

To obtain rough estimates, the condition that the planet's gravity be strong enough to overwhelm pressure in its neighbourhood is that the radius of the Hill sphere exceeds the disk semi-thickness and that the viscous stresses are overwhelmed by planetary tides. For details on gap opening see the review by Lin & Papaloizou

(1993), and also Bryden et al. (1999); Kley (1999). For planetary masses large enough to open a gap the migration rates are no longer given by the linear estimates but will have to be calculated through numerical simulations. The resulting migration is called Type II migration.

3.2.1 Numerical Modeling

The first modern high-resolution hydrodynamical calculations of planet-disk interaction have been performed by Kley (1999), Bryden et al. (1999), Lubow et al. (1999), and Nelson et al. (2000). Since protoplanetary accretion disks are assumed to be vertically thin, these first simulations use a two-dimensional ($r-\varphi$) model of the accretion disk. The vertical thickness H of the disk is incorporated by assuming a given radial temperature profile $T(r) \propto r^{-1}$ which makes the ratio H/r constant. Typically the simulations assume $H/r = 0.05$ which refers to a disk where at each radius the Keplerian speed is 20 times faster that the local sound speed. Initial density profiles typically have power laws for the surface density $\Sigma \propto r^{-s}$ with s between 0.5 and 1.5. Later also fully 3D models have been calculated which still use a simple isothermal equation of state (D'Angelo et al. 2003; Bate et al. 2003).

For the anomalous viscosity of accretion disks a Reynolds stress tensor formulation (Kley 1999) is used typically where the kinematic viscosity ν is either constant or given by an α-prescription $\nu = \alpha c_s H$, where α is constant and c_s is the local sound speed. From observations, values lying between 10^{-4} and 10^{-2} are inferred for the α-parameter of protoplanetary disks. Full MHD-calculations have shown that the viscous stress-tensor ansatz may give (for sufficiently long time averages) a reasonable approximation to the *mean* flow in a turbulent disk (Papaloizou & Nelson 2003). The embedded planets are assumed to be point masses (using a smoothed potential), and together with the star they are treated as a classical N-body system. The disk also influences the orbits through the gravitational torques. This is the desired effect to be studied which will cause the orbital evolution of the planets. The planets may also accrete mass from the surrounding disk (Kley 1999).

To enhance resolution in the vicinity of the planet, the computations are typically performed in a rotating frame. Numerically, a special treatment of the Coriolis force has to be incorporated to ensure angular momentum conservation (Kley 1998).

3.2.2 Viscous laminar Disks

The type of modeling outlined in the previous section yields in general smooth density and velocity profiles, and we refer to those models as *viscous laminar disk* models, in contrast to models which do not assume an a priori given viscosity and rather model the turbulent flow directly.

A typical result of such a viscous computation obtained with a 128×280 grid (in $r-\varphi$) is displayed in Fig. 3. Here, the planet with mass $M_p = 1 M_{\rm Jup}$ and semi-major axis $a_p = 5.2$AU is *not* allowed to move and remains on a fixed circular orbit, an approximation which is typical in many simulations. Clearly seen are the major effects an embedded planet has on the structure of the protoplanetary accretion disk. The gravitational force of the planet leads to a spiral wave pattern in the disk.

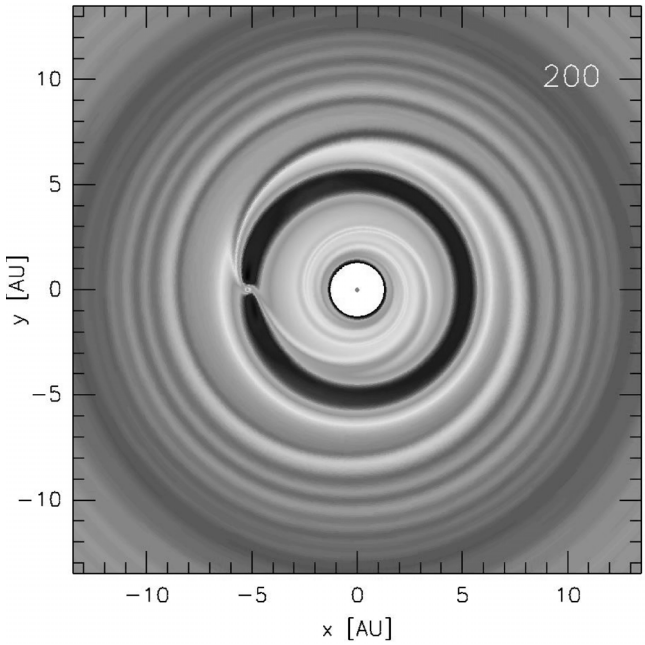

Figure 3: Surface density profile for an initially axisymmetric planet-disk model with $M_{Planet} = 1 M_{\rm Jup}$ after 200 orbital periods of the planet.

In the present calculation (Fig. 3) there are two spirals in the outer disk and in the inner disk. This is because the edge of the gap lies at that distance from the planet where $m = 2$ spiral arms are created. A variation of the sound speed in the disk may change the number of launched spirals (Kley 1999). The tightness of the spiral arms depends on the temperature (i.e. H/r) of the disk. The smaller the temperature the tighter the spirals.

The second prominent feature is the density gap at the location of the planet. It is caused by the deposit of positive (at larger radii) and negative (at smaller radii) angular momentum in the disk. The spiral waves are corotating in the frame of the planet, and hence their pattern speed is faster (outside) and lower (inside) than the disk material (see Sect. 3.1). Dissipation by shocks or viscosity leads to the deposit of this angular momentum, which pushes material away from the planet. The equilibrium width of the gap is determined by the balance of gap-closing viscous and pressure forces and gap-opening gravitational torques. For typical parameter of a protoplanetary disk, a Saturn mass planet will begin to open a visible gap. More explicit details on gap opening criteria are given in the review by Lin & Papaloizou (1993), and see also Bryden et al. (1999).

In Fig. 4 the density structure and flow field in the immediate vicinity of the planet is plotted. The shock-wave character of the trailing inner and outer spiral arms is clearly visible. Upstream material enters the Roche-lobe from the inside and

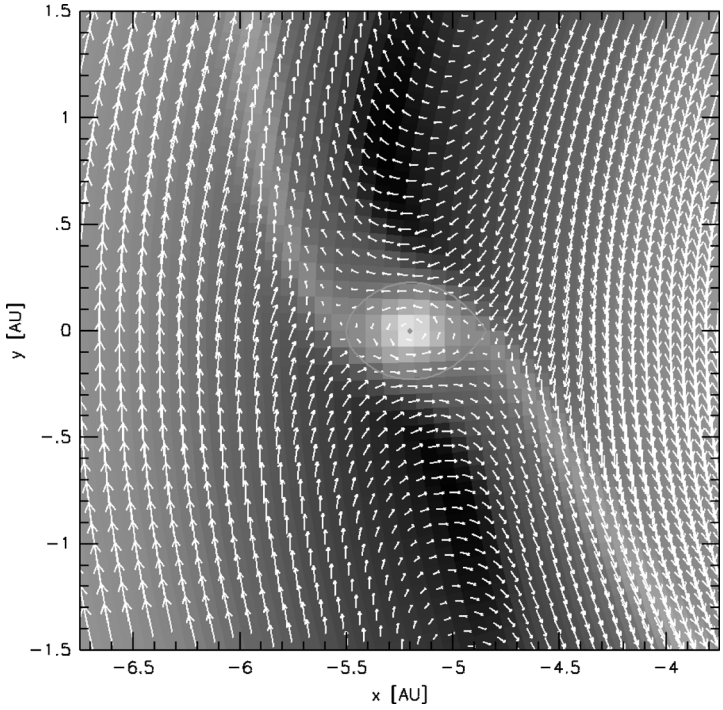

Figure 4: Flow field in the vicinity of a Jupiter mass planet (after Kley (1999)).

outside and can be accreted onto the planet. Around the planet a circumplanetary accretion disk is formed. As may be inferred from the flow field, a Jupiter mass planet is still able grow in mass. Only for a mass about 5 $M_{\rm Jup}$ the gap width begins to deepens sufficiently to essentially limit further accretion onto the planet. The planetary masses reachable via disk accretion nevertheless is beyond that what has been estimated previously from simple gap opening criteria. Hence, through this mechanism the large masses of the extrasolar planets can be explained easily. The sense of the rotation of the circumplanetary disk inside the Roche lobe of the planet is prograde, explaining naturally the observed preference of prograde rotation in our Solar System.

To obtain more insight into the flow near the planet and to calculate accurately the torques of the disk acting on the planet, a much higher spatial resolution is required. As this is necessary only in the immediate surrounding of the planet, a number of nested-grid and also variable grid-size simulations have been performed (D'Angelo et al. 2002, 2003; Bate et al. 2003). Such a grid-system is not adaptive, as it is defined in the beginning of the computation and does not change with time. The planet is placed in the center of the finest grid.

The result for a 2D computation using 6 grids is displayed in Fig. 5, for more details see also D'Angelo et al. (2002). The top left base grid has a resolution of 128×440 and each sub-grid has a size of 64×64 with a refinement factor of two from

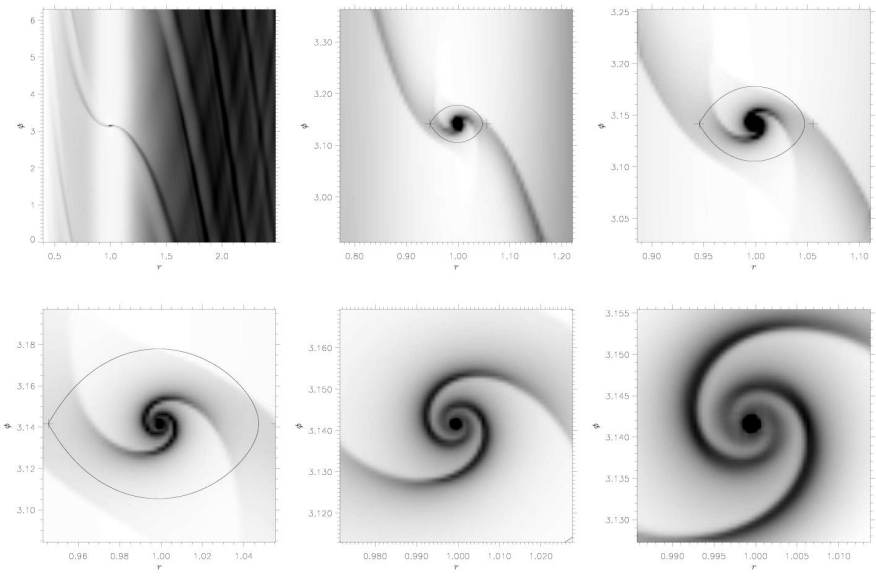

Figure 5: Density Structure of a $1M_{\rm Jup}$ on each level of the nested grid system, consisting of 6 grid levels in total. The top left panel displays the total computational domain. The line indicates the size of the Roche lobe (after D'Angelo et al. (2002).

level to level. It is noticeable that the spiral arms inside the Roche-lobe of the planet are detached from the global outer spirals. The two-armed spiral around the planet extends deep inside the Roche-lobe and allows for the accretion of material onto the planet. The nested-grid calculations have recently been extended to three dimensions (3D) and a whole range of planetary masses have been investigated, starting from 1 Earth mass to a few Jupiter masses (Kley et al. 2001; D'Angelo et al. 2003). In the 3D case the strength of the spiral arms are weaker and accretion occurs primarily from regions above and below the midplane of the disk.

From the density distribution the forces acting on the planet can be calculated directly, and the migration time scale be estimated. The results obtained for small and large planetary masses are given in Fig. 2. The results for small and intermediate masses have been discussed already in Sect. 3.1. The general trend is an increase in the migration rate because of the increased planetary mass (see also Eq. (2)), interrupted only by the described *dip* for intermediate masses. The turnover in the migration rate for larger masses is due to the limiting behaviour of the viscosity. The inward migration rate cannot be larger than the viscous (inward) motion of the disk as otherwise the planet may loose contact to the disk and cease migration. Hence, for larger masses the migration rate is given by the viscously evolving disk (so called *Type II migration*). The migration time scale for Jupiter type planets in the Type II regime is approximately given by 10^5yrs for typical disk parameter. For even larger masses the increased inertia of the planet slows it down even further (Ivanov et al. 1999).

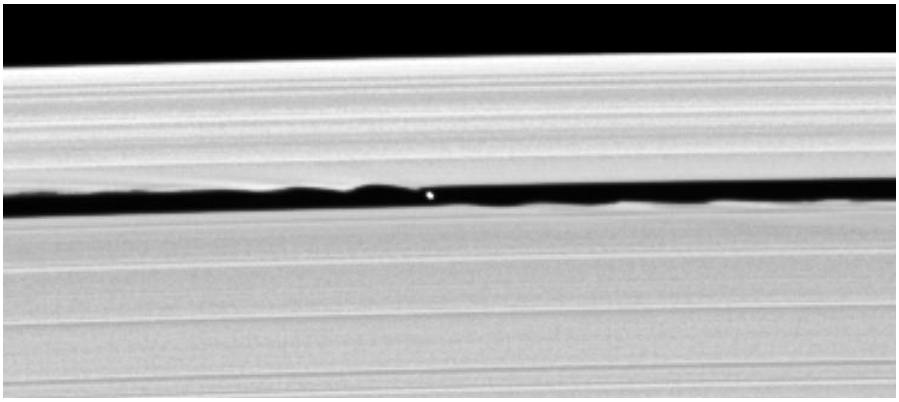

Figure 6: The Saturnian moon (S/2005 S1) within the Keeler gap as discovered by the Cassini mission. Clearly visible are the wavelike disturbances at the gap edges created by the satellite. The gap has a width of 40 km and the moon a diameter of about 7 km. (Courtesy of ESA/JPL)

The inward motion and accretion of the planet has been followed directly by releasing the assumption of a fixed planet and rather evolve its orbital elements and mass accretion directly simultaneously during the hydrodynamic evolution. The fully non-linear simulations confirm the above estimates and show that a Jupiter type planet may reach approach the central star within roughly 10^5yrs while growing upto 5 $M_{\rm Jup}$ on its inward journey (Nelson et al. 2000). This inward migration scenario of embedded planets is presently the favoured explanation for the origin of the population of so-called hot Jupiters, i.e. massive planets which orbit their star with periods of only a few days.

It is well known that moons embedded in Saturns rings have a strong dynamical influence on the dynamics of the disk. Even though the Saturnian ring system consists of an ensemble of solid particles, the dynamical evolution is in fact very reminiscent to what happens in a protoplanetary disk, only the effect of spiral arms which are clearly due to pressure and sound wave effects are not visible in Saturn's rings. In particular the feature of well defined gaps within the rings has been attributed to the presence of moons within the gaps. Due to their faintness however, only very few have been detected directly from earth. Now, the Cassini space mission to Saturn has provided recently additional nice evidence for gap formation in our Solar System in the form of the moon S/2005 S1 which lies exactly within the Keeler gap of the Saturn's rings (see Fig. 6). To observe gaps in protoplanetary disks carved by young planets one has to wait for the advent of sensitive instruments with high resolution in the IR, such a ALMA. A prospective study of what to expect for such a case has been performed already by Wolf et al. (2002).

Table 1: Orbital parameters of the two resonant planets of the planetary system GJ 876 at epoch JD 2449679.6316 assuming co-planarity and $i = 90^\circ$ as given by Laughlin et al. (2004). The adopted stellar mass is $M_* = 0.32\mathrm{M}_\odot$. P denotes the orbital period, M the mass of the planet, a the semi-major axis, e the eccentricity, ϖ the angle of periastron at epoch, and q the mass ratio M/M_*. The innermost planet d is not listed.

	P [d]	M [$M_{\rm Jup}$]	a [AU]	e	ϖ [deg]	q [10^{-3}]
Inner	30.38	0.597	0.13	0.218	154	1.78
Outer	60.93	1.89	0.21	0.029	149	5.65

4 Resonant Planets

4.1 Observations

Among the 15 known extrasolar planetary systems with multiple planets, possibly five exhibit pairs of planets that are likely to be in orbital resonances at low order commensurabilities of their mean motions. The pair of planets around GJ 876 (Marcy et al. 2001) is well confirmed to be deep in the resonances associated with the 2:1 mean motion commensurability (Laughlin & Chambers 2001; Rivera & Lissauer 2001; Laughlin et al. 2004), where resonant angles $\theta_1 = 2\lambda_2 - \lambda_1 - \varpi_1$, $\theta_2 = 2\lambda_2 - \lambda_1 - \varpi_2$, and $\Delta\varpi = \varpi_2 - \varpi_1 = \theta_1 - \theta_2$ are all librating about 0° with small amplitudes. Here λ_j are mean longitudes and ϖ_j are longitudes of periapse, both numbered from the inside out. The pair of planets around HD 82943 is likely to also be in resonances at 2:1 (Mayor et al. 2004), and the middle pair of planets in the 4 planet system orbiting 55 Cnc may be in resonances at 3:1 (Marcy et al. 2002; McArthur et al. 2004). Thus as many as one-fourth of the known multiple-planet systems contain planets in mean motion resonances. An overview of the parameter of the resonant pair of planets within the system GJ 876 is given in Table 1, the newly discovered innermost planet Rivera et al. (2005) is not listed because due to its closeness to the star, it does not influence the behaviour of the resonant pair.

4.2 The Hydrodynamical Model

In case of simulations of resonant planetary systems the models are calculated very similar to those described above for single planets (Kley 1998, 1999). The first hydrodynamical simulations of a multiple system has been presented in Kley (2000). The reader is referred to those papers for details on the computational aspects of this type of simulations. Other similar models, following explicitly the motion of single and multiple planets in disks, have been presented by Nelson et al. (2000), Bryden et al. (2000), Snellgrove et al. (2001), Papaloizou (2003), and in more detail recently for resonant configurations by Kley et al. (2004).

For the case of two planets the typical evolutionary state of the disk (containing the planets) is given in Fig. 7. Due to the different orbital velocities of the planets

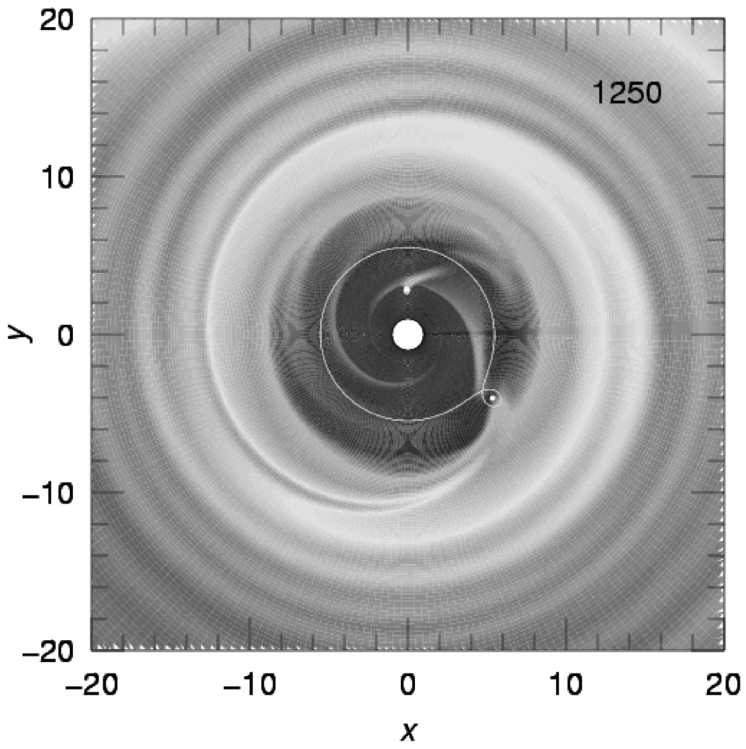

Figure 7: Overview of the density distribution of an embedded pair of planets after 1250 orbital periods of the inner planet. Higher density regions are brighter and lower ones are darker. The star lies at the center of the white inner region bounded by $r_{min} = 1$ AU. The location of the two planets is indicated by the white dots, and their Roche-lobes are also drawn.

there exists no co-rorating frame with stationary spiral arms. Caused by this strong time variations of the flow the region in between the planets clears relatively rapidly (within around 500–1000 orbits of the inner planet), and a configuration such as shown in Fig. 7 where two planets orbit within a large gap (or rather hole) in the protoplanetary disk is created. The clearing of disk material between two planets both capable of opening a gap in the disk leads to *differential migration* of the two planets as the outer planet is forced in by the material remaining outside its orbit, while the inner planet is stalled. The convergence of the orbits naturally allows capture into stable resonant orbital configurations. Hydrodynamical simulations of two embedded planets capturing each other into resonance have been performed by several groups (Kley 2000; Bryden et al. 2000; Snellgrove et al. 2001; Papaloizou 2003; Kley et al. 2004). The resonance capture has also been analyzed with extensive three-body calculations, where migration is simply imposed with either the semi-major axis mi-

gration rate $\dot{a}/a$ and the eccentricity damping rate $\dot{e}/e$ specified explicitly or ad hoc forces added to produce migration and eccentricity damping (Snellgrove et al. 2001; Lee & Peale 2002; Nelson & Papaloizou 2002; Kley et al. 2004; Lee 2004).

In a recent paper Kley et al. (2005) analyzed in detail the formation of the resonant planetary system GJ 876 for which, due the relatively short periods of the two planets, the determination of orbital parameters is by far the most accurate (see Table 1). As mentioned, the system is deep in the 2:1 resonance where both resonant angles Θ_1 and $\Delta\varpi$ are librating around 0° with maximum amplitudes of $|\Delta\varpi|_{max}$ = 34° and $|\Delta\Theta_1|_{max}$ = 7°. The peri-astron shift is retrograde and amounts to 41°/yr.

Having in mind the typical geometry in a resonant planetary system (see Fig. 7) the numerical effort has been optimized, such that only the outer planet moves inside the computational domain (see Fig. 8). This approach is appropriate since only the outer planet is still in touch with the the ambient disk while the inner planet is orbiting in an inner hole of the disk with only little mass surrounding it. The two-dimensional fully non-linear hydrodynamic simulations include viscous heating, radiative transport in the midplane of the disk and vertical radiative cooling. To model disk dispersal mass has been taken out slowly from the outer region of the disk. For the numerical details and the model setup see Kley et al. (2005).

4.3 Modeling the evolution of GJ 876

The evolution of the semi-major axis and eccentricities is given in the top panel of Fig. 9. Initially only the outer planet (index 2, light gray curves) migrates inward while the inner planet does not migrate appreciably. After around 400 yrs the outer planet has begins to capture the inner planet in the 2:1 resonance. From then on the two planets migrate inwards together always keeping their 2:1 resonant condition. Upon resonant capture both eccentricities rise, that of the inner planet up to $e_1 = 0.26$, and that of the outer planet to $e_2 = 0.04$. Due to the disk dispersal the inward migration is essentially halted after around 2000 yrs. To speed up the evolution (driving) of this system, the viscosity and the disk mass have been chosen larger than what is typically assumed for protoplanetary disks. However, as shown for example by Lee & Peale (2002) the final state of the system does not depend on the assumed speed of migration but is rather given by the physical parameter (masses) of the involved planets. The final values of the eccentricities obtained in the hydrodynamic simulations (Fig. 9) are in very good agreement with the observed values of GJ 876 (Table 1).

Upon capture the apsidal lines of the two planets first align in the anti-symmetric state where the periastrae are separated by $\Delta\varpi = 180^\circ$. Further evolution however, leads to the described increase of eccentricities and the system adjusts after around 1400–1500 yrs to the symmetric case with $\Delta\varpi = 0^\circ$ (Fig. 9, bottom right). The libration angle is slowly decreasing and at the end of the simulation the system has reached approximately $|\Delta\varpi|_{max} = 50^\circ$ in rough agreement with the observed value of 34°. The corresponding resonant angle Θ_1 begins to librate around 0° very fast and the libration amplitude has declined during the evolution to about $|\Delta\Theta_1|_{max} = 30^\circ$ somewhat larger than the observed value of 7°. However, in general the final state of the system matches the observed values quite well.

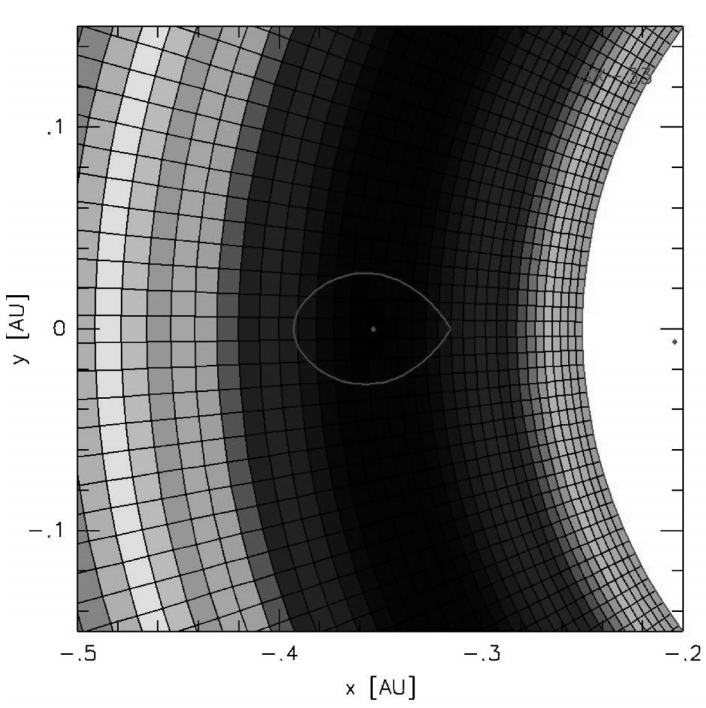

Figure 8: Part of the numerical grid used by Kley et al. (2005) for the simulations of resonant system GJ 876. Only the outer planet moves within the computational domain. Shown is also the size of the Roche lobe for the outer planet with the mass ratio $q = 0.0059$. The inner planet with $q = 0.00175$ is located inside of the computational domain and is just visible in the center on the right hand side. The gray scale shading gives the initial profile of the surface density.

5 Summary

We have shown that observationally there is now ample evidence for the existence of protoplanetary disks around young stars with an age younger than about 10^7 yrs. These disks are seen in the SED, can directly imaged and their existence can be inferred indirectly by polarization measurements. From spectral measurements and direct imaging at different wavelengths evidence for grain growth has been inferred. New observations obtained by the Spitzer space telescope confirm the existence of inner holes in these disks with an extend of several AU. This is often taken as evidence for the presence of a (massive) planet which truncates the disk and prevents further mass accretion onto the star.

The fully non-linear hydrodynamical calculations for Jupiter-sized planets embedded planets have shown that disk-planet interaction has the following general properties.

- The excitation of spiral shock waves in the disk, whose tightness depends on the sound-speed in the disk. Higher disk temperatures yield wider spirals while small temperature show tightly wound spirals.
- The formation of an annular gap, whose width is determined by the balance between gap-opening tidal torques and gap-closing viscous plus pressure forces.
- An inward migration on a time scale of 10^5 yrs for typical disk parameters, in particular disk masses corresponding to that of the minimum mass solar nebula.
- A possible mass growth after gap formation up to about 5–10 $M_{\rm Jup}$ when finally the gravitational torques overwhelm the diffusive tendencies of the gas.
- A prograde rotation of the planet.

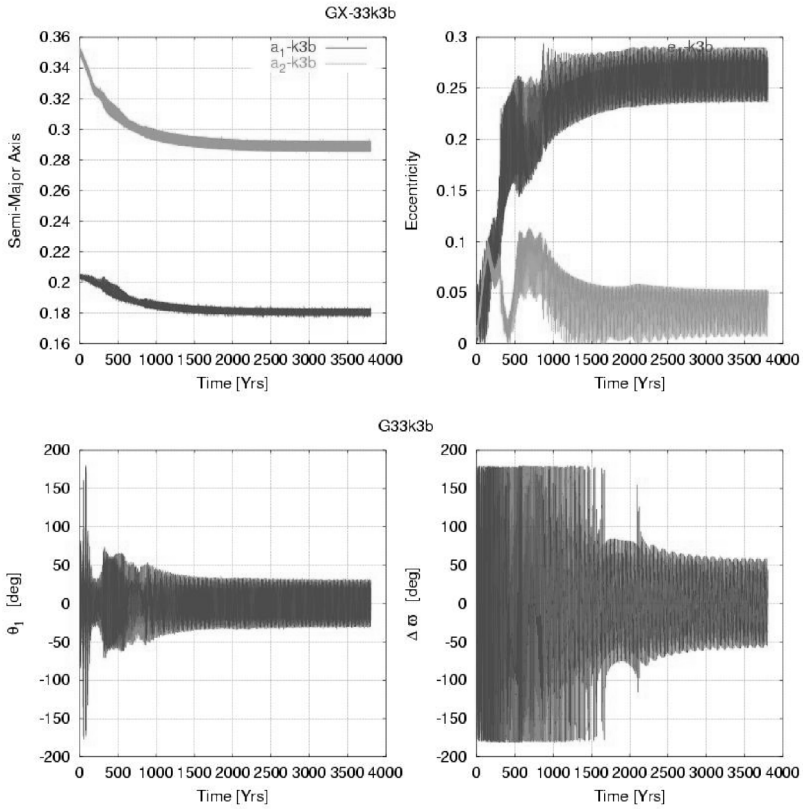

Figure 9: Top: The evolution of the semi-major axis a and the eccentricity e of a pair of planets having initially the semi-major axis of 0.2 and .35 AU and eccentricities of 0.01 each. **Bottom**: Evolution of the resonant angles Θ_1 and $\Delta\varpi$ during the evolution.

From the evolution of the resonant system GJ 876 we can draw important conclusions on issues such as migration and eccentricity behaviour.

- As the resonant state can only be reached through differential motion of two planets, it represents besides the existence of hot Jupiters the strongest evidence that disk induced migration has indeed occurred during the early evolution of planetary systems.

- In the case of inward migration where the outer planet is still in touch with the outer disk we expect that it will have a higher mass than the inner planet, a fact which is definitely true for GJ 876 and probably also for other systems.

- It has been suggested (Goldreich & Sari 2003) that planet disk interaction may raise the eccentricities of the planets and be an explanation for the observed eccentricity distribution of extrasolar planets. A subject presently under active investigation because numerical hydrodynamical evolutions do in general find eccentricity damping by the disk. One major problem in models for the evolution of GJ 876 has always been the fact that the observed eccentricities are very small considering the strong increase in eccentricities occurring during resonant capture. As shown previously (Lee & Peale 2002; Kley et al. 2004) these can only be explained by assuming an eccentricity damping timescale much shorter than the migration scale. An excitation of eccentricity by planet disk interaction would make the problem even worse. This conclusion is confirmed by a recent analysis of the planetary system υ And where the observed eccentricities can be best explained by a more abrupt scattering process rather than by secular planet-disk interaction (Ford et al. 2005).

- As shown in the most recent simulations Kley et al. (2005) in addition to the damping of eccentricity also disk dispersal has probably taken into account. The inferred disk dissipation timescale has to be of the order of the migration timescale. Only then the driving force is reduced rapidly enough to limit the growth of eccentricities to the observed values.

A possible new type of migration (Type III) has been found for planets partially depleting their co-orbital region in massive disks. In this case a positive feedback between the planet migration rate and the so-called corotation torque (the latter increasing with the former) may lead to runaway migration. A discussion of this process has not been part of this review, but see Masset & Papaloizou (2003); Masset & Ogilvie (2004) and the recent review by Masset & Kley (2005) on the topic of disk-planet interaction.

The existence of a diffusive migration mode of small mass objects in disks invaded by the magneto-rotational instability has been observed in heavy numerical MHD simulations. Detailed predictions on the efficiency and direction of migration still remain an open issue. This type stochastic mode of migration has also not been covered in this review but see Nelson & Papaloizou (2004) and the references therein.

Understanding the formation and evolution of planetary systems has seen a revival of scientific interest and has been in the center of astrophysical research during

the past years, and many facets of this highly interesting and complex topic remain to be studied in the future.

Acknowledgements

I would like to thank my colleagues Doug Lin, Richard Nelson, Frederic Masset, John Papaloizou and many others for all the stimulating and interesting discussions and interactions during the last years. The work on the system GJ 876 was sponsored by the KITP Program "Planet Formation: Terrestrial and Extra-Solar" held in Santa Barbara from January 2004 until March 2004. I thank the organizers for providing a pleasant and very stimulating atmosphere. Part of the work was sponsored by the EC-RTN Network *The Origin of Planetary Systems* under grant HPRN-CT-2002-00308.

References

Alibert, Y., Mordasini, C., & Benz, W. 2004, A&A, 417, L25

Bate, M. R., Lubow, S. H., Ogilvie, G. I., & Miller, K. A. 2003, MNRAS, 341, 213

Bell, K. R. & Lin, D. N. C. 1994, ApJ, 427, 987

Briceño, C., Vivas, A. K., Calvet, N., et al. 2001, Science, 291, 93

Bryden, G., Chen, X., Lin, D. N. C., Nelson, R. P., & Papaloizou, J. C. B. 1999, ApJ, 514, 344

Bryden, G., Różyczka, M., Lin, D. N. C., & Bodenheimer, P. 2000, ApJ, 540, 1091

Calvet, N., D'Alessio, P., Hartmann, L., et al. 2002, ApJ, 568, 1008

Chiang, E. I. & Goldreich, P. 1997, ApJ, 490, 368

D'Alessio, P., Calvet, N., Hartmann, L., Lizano, S., & Cantó, J. 1999, ApJ, 527, 893

D'Alessio, P., Canto, J., Calvet, N., & Lizano, S. 1998, ApJ, 500, 411

D'Angelo, G., Henning, T., & Kley, W. 2002, A&A, 385, 647

D'Angelo, G., Kley, W., & Henning, T. 2003, ApJ, 586, 540

Dullemond, C. P., Dominik, C., & Natta, A. 2001, ApJ, 560, 957

Dullemond, C. P. & Natta, A. 2003, A&A, 405, 597

Edwards, S., Cabrit, S., Strom, S. E., et al. 1987, ApJ, 321, 473

Ford, E. B., Lystad, V., & Rasio, F. A. 2005, Nature, 434, 873

Goldreich, P. & Sari, R. 2003, ApJ, 585, 1024

Goldreich, P. & Tremaine, S. 1979, ApJ, 233, 857

Hartmann, L., Kenyon, S. J., & Calvet, N. 1993, ApJ, 407, 219

Ivanov, P. B., Papaloizou, J. C. B., & Polnarev, A. G. 1999, MNRAS, 307, 79

Kley, W. 1998, A&A, 338, L37

Kley, W. 1999, MNRAS, 303, 696

Kley, W. 2000, MNRAS, 313, L47

Kley, W., D'Angelo, G., & Henning, T. 2001, ApJ, 547, 457

Kley, W., Lee, M. H., Murray, N., & Peale, S. J. 2005, A&A, 437, 727

Kley, W., Peitz, J., & Bryden, G. 2004, A&A, 414, 735

Laughlin, G., Butler, R. P., Fischer, D. A., et al. 2004, astro-ph/0407441, ApJ, in press

Laughlin, G. & Chambers, J. E. 2001, ApJ, 551, L109

Lee, M. H. 2004, ApJ, 611, 517

Lee, M. H. & Peale, S. J. 2002, ApJ, 567, 596

Lin, D. N. C. & Papaloizou, J. C. B. 1980, MNRAS, 191, 37

Lin, D. N. C. & Papaloizou, J. C. B. 1993, in Protostars and Planets III, 749–835

Lissauer, J. J. 1993, ARA&A, 31, 129

Lubow, S. H., Seibert, M., & Artymowicz, P. 1999, ApJ, 526, 1001

Malfait, K., Waelkens, C., Waters, L. B. F. M., et al. 1998, A&A, 332, L25

Marcy, G. W., Butler, R. P., Fischer, D. A., et al. 2002, ApJ, 581, 1375

Marcy, G. W., Butler, R. P., Fischer, D. A., et al. 2001, ApJ, 556, 296

Masset, F., D'Angelo, G., & Kley, W. 2006, in preparation,

Masset, F. & Kley, W. 2005, in Planet Formation: Theory, Observations and Experiment, ed. H. Klahr & W. Brandner, Vol. in press.

Masset, F. S. & Ogilvie, G. I. 2004, ApJ, 615, 1000

Masset, F. S. & Papaloizou, J. C. B. 2003, ApJ, 588, 494

Mayor, M., Udry, S., Naef, D., et al. 2004, A&A, 415, 391

McArthur, B. E., Endl, M., Cochran, W. D., et al. 2004, ApJ, 614, L81

McCaughrean, M. J., Stapelfeldt, K. R., & Close, L. M. 2000, Protostars and Planets IV, 485

Meyer-Vernet, N. & Sicardy, B. 1987, Icarus, 69, 157

Nelson, R. P. & Papaloizou, J. C. B. 2002, MNRAS, 333, L26

Nelson, R. P. & Papaloizou, J. C. B. 2003, MNRAS, 339, 993

Nelson, R. P. & Papaloizou, J. C. B. 2004, MNRAS, 350, 849

Nelson, R. P., Papaloizou, J. C. B., Masset, F. S., & Kley, W. 2000, MNRAS, 318, 18

Papaloizou, J. & Lin, D. N. C. 1984, ApJ, 285, 818

Papaloizou, J. C. B. 2003, Celestial Mechanics and Dynamical Astronomy, 87, 53

Papaloizou, J. C. B. & Nelson, R. P. 2003, MNRAS, 339, 983

Papaloizou, J. C. B. & Nelson, R. P. 2005, A&A, 433, 247

Rivera, E. J. & Lissauer, J. J. 2001, ApJ, 558, 392

Rivera, E. J., Lissauer, J. J., Butler, R. P., et al. 2005, ApJ, 634, 625

Shuping, R. Y., Bally, J., Morris, M., & Throop, H. 2003, ApJ, 587, L109

Snellgrove, M. D., Papaloizou, J. C. B., & Nelson, R. P. 2001, A&A, 374, 1092

Strom, K. M., Strom, S. E., Edwards, S., Cabrit, S., & Skrutskie, M. F. 1989, AJ, 97, 1451

Tanaka, H., Takeuchi, T., & Ward, W. R. 2002, ApJ, 565, 1257

Ward, W. R. 1986, Icarus, 67, 164

Ward, W. R. 1997, Icarus, 126, 261

Wilner, D. J. & Lay, O. P. 2000, Protostars and Planets IV, 509

Wolf, S., Gueth, F., Henning, T., & Kley, W. 2002, ApJ, 566, L97

Wolf, S., Padgett, D. L., & Stapelfeldt, K. R. 2003, ApJ, 588, 373

Zinnecker, H., Krabbe, A., McCaughrean, M. J., et al. 1999, A&A, 352, L73